Residual stress relaxation induced by shot peening in Inconel® 718 under quasi-static and cyclic loading

J. Hoffmeister[1], V. Schulze[1], R. Hessert[2], G. Koenig[2]

1 Institute for applied materials (IAM), Karlsruhe Institute of Technology (KIT), Kaiserstr. 12, 76131 Karlsruhe, Germany
2 MTU Aero Engines, Dachauer Str. 665, 80995 Munich, Germany

Abstract

Shot peening is often used to improve the fatigue life of turbine components. Therefore it is very important to know the changes of the residual stress state due to quasi-static and cyclic loading. The objective of this work was to describe the residual stress state in the nickel base forge alloy Inconel® 718 (IN718) induced by shot peening after a quasi-static and cyclic loading. In order to find out the changes of the residual stresses after quasi-static loading, different shot peened specimens were loaded isothermally up to a specific tensile loading. To describe the residual stress state after cyclic loading isothermal low cycle fatigue tests were performed. These tests were stopped after a specific number of cycles. After the different loadings the residual stresses at the surface and for special loadings the residual stress depth distributions were determined experimentally by using X-ray diffraction.

Based on the surface-core-model, the deformation behaviour of the surface can be deduced from the results of the quasi-static experiments. The model was expanded to a multi-layer model so that the complete residual stress distribution after quasi-static loading can be described. The residual stresses after cyclic loading are not dependent on the number of cycles so that the quasi-static model can be applied also for cyclic residual stress changes.

Keywords: Inconel® 718, IN718, nickel base alloy, residual stresses, stability

Introduction

Shot peening can significantly increase the fatigue life of turbine components. The improvement of the properties can be attributed to near-surface residual stresses and work hardening. Because turbine engines work at high temperatures and under mechanical load, the positive effects on the mechanical properties can be reduced by the thermal and mechanical relaxation of residual stresses. For the design of turbines it is therefore very important to know the dependence of the stress relaxation on the temperature and the mechanical loading. In this paper the mechanical macro residual stress relaxation of IN718 was investigated under isothermal quasi-static and cyclic loading. After the mechanical loading conditions were applied X-ray stress analyses were performed and the experimental results were modeled.

Methods

The investigations were carried out on age hardened IN718 round specimens. The diameters of the samples were 7 mm and the gauge lengths 26 mm. The cylindrical surfaces of the samples were shot peened with an Almen intensity of 0.25 mmA.

In order to find out the change of the quasi-static residual stresses, interrupted tensile tests were performed. Therefore, different specimens were isothermally (testing temperature TT < 650 °C) loaded for different total strains between 0 % and 2.5 %.

To describe the residual stress state after cyclic loading isothermal (testing temperature TT < 650 °C) low cycle fatigue tests which were stopped after a specific number of cycles were performed. The total strain amplitude varied between 0.35 % and 0.6 % at fixed load ratio R = 0.

The surface residual stresses were measured before and after the mechanical treatment by X-ray diffraction on the {311}-interference using Mn-Kα-radiation and evaluated using the $\sin^2\psi$-method applying a Young's modulus of $E^{\{311\}}$=200 GPa, a Poisson's ratio of $\nu^{\{311\}}$=0.32 and a stress-free diffraction angle $2\theta_0^{\{311\}}$=151°.

For selected mechanical loadings the complete depth distributions of residual stresses were measured by alternating electro polishing and measuring steps. Because the removed area was small, the stress relaxation could be ignored.

Experimental Results

The residual stresses after different quasi-static loads are shown in Figure 1 (left). The surface residual stresses relax due to the thermal load [1] (Temperature T3 in [1] correlates to the testing temperature TT). After this the residual stresses are nearly constant until the total strain achieves the elastic limit. Now the compressive residual stresses decrease until tensile residual stresses build up. The depth distributions of residual stresses (cf. Figure 5 (left)) show the same behavior at and near the surface. For depths greater than the depth of the maximum compressive residual stresses, the residual stresses do not cross the zero line. It can also be seen that the depths of the maximum and the zero-crossing of the residual stresses are almost constant.

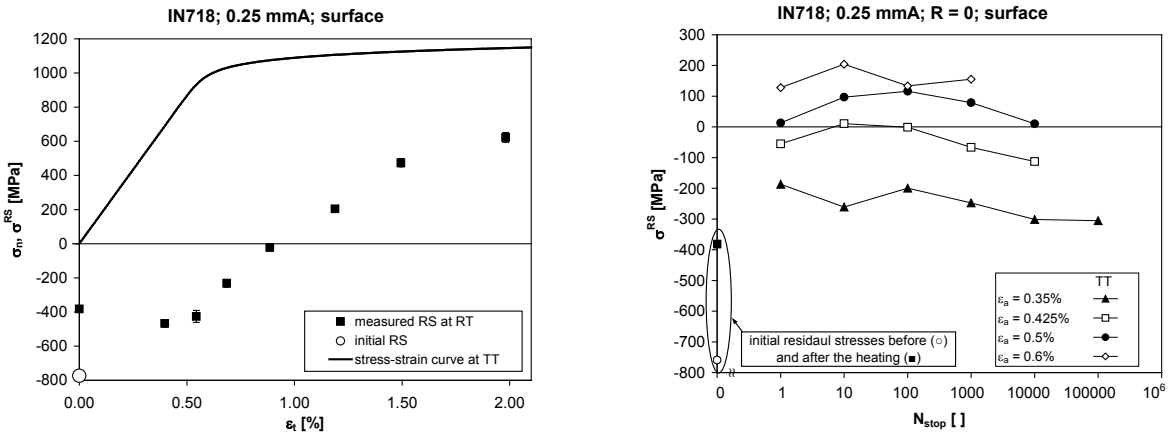

Figure 1: Influence of the quasi-static (left) and the cyclic (right) mechanical load on the surface residual stresses

After one cycle of cyclic loading (cf. Figure 1 (right)) the surface residual stresses show the same behaviour like the ones of quasi-static loading. First the residual stresses relax because of the thermal loading. Then the compressive residual stresses relax until tensile residual stresses are built up. Looking at all cycle numbers, the surface residual stresses remain nearly constant. In Figure 5 (right) the depth distributions of residual stresses are shown after different cyclic loading. The depth distributions show the same behavior like those after quasi-static loading.

Discussion

The surface-core-model [2,3] is the basic for modelling the isothermal quasi-static relaxation of residual stresses. Because the residual stresses (at room temperature RT) and the stress strain-curve (at testing temperature TT) are measured at different temperatures, the residual stresses must be converted to the testing temperature TT. Therefore residual stresses,

which are correlating with elastic strains, are multiplied with the ratio of Young's modulus at testing temperature E(TT) and Young's modulus at room temperature E(RT).

$$\sigma^{RS}(T3) = \sigma^{RS}(RT) \cdot \frac{E(TT)}{E(RT)} \tag{1}$$

This residual stresses at testing temperature (TT) (cf. Figure 2) are added on the stresses of the stress-strain curve at corresponding strain values. As a result, there are supporting points to fit the stress-strain curve of the surface.

Therefore, an approach where the negative stress values are described with Hooke's law which starts at the residual stresses at the beginning of the mechanical loading ${\sigma_O}^{RS}$ and the positive stress values are described with a Ramberg-Osgood-approach [4] which is shifted to the end of Hooke's line is the basis for the description of the stress-strain curve of the surface:

$$\begin{aligned} \varepsilon_t &= \frac{\sigma - {\sigma_O}^{RS}(\varepsilon_t = 0, TT)}{E} && \text{for } \sigma \le 0 \\ \varepsilon_t &= \frac{\sigma - {\sigma_O}^{RS}(\varepsilon_t = 0, TT)}{E(TT)} + \left[\frac{\sigma}{K_{surface}}\right]^{1/n_{surface}} && \text{for } \sigma > 0 \end{aligned} \tag{2}$$

The stress-strain curve of the surface and its location is described completely by the strain hardening coefficient $K_{surface}$, the strain hardening exponent surface $n_{Surface}$, the Young's modus E(TT) at testing temperature and the residual stresses at the beginning of the mechanical loading ${\sigma_O}^{RS}$. With this approach and the aid of a least-square-algorithm the stress-strain curve of the surface can be fitted to supporting points (cf. Figure 2 red line).

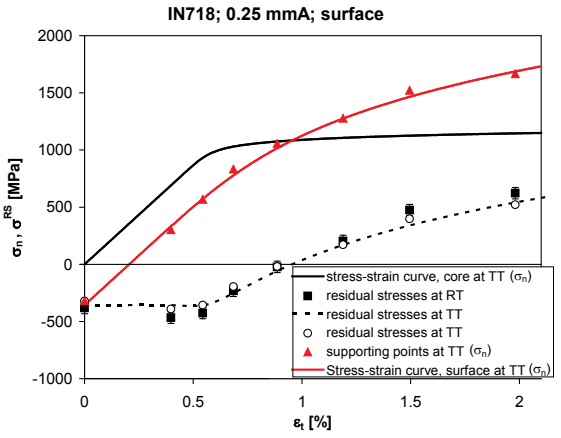

Figure 2: Procedure to discribe the surface residual stresses as function of total strain

To get the residual stresses at testing temperature as a function of the total strain, the stress-strain curve of the core material must be subtracted from the stress-strain curve of the surface. Finally, the residual stresses at testing temperature must be divided by the ratio of the Young's modulus (cf. equation (1)) to get the residual stresses at room temperature (cf. Figure 2 dash line).

This procedure makes a good description of the residual stress relaxation at the surface. But it isn't possible to describe the whole residual stress distribution as a function of the applied total strain under quasi-static loading.

Therefore, the measured residual stress depth distributions are divided into different depth layers with a distance of 40 µm (cf. Figure 3 (left)). With the four residual stress distributions for the applied total strains ε_t = 0 %; 0.7 %; 1.2 % and 2 % resulting in four residual stress values for each depth layer (cf. Figure 3 left, encircled intersection points). With these four residual stress values for every depth layer it is possible to describe the residual stress relaxation with the same procedure as for the surface: the residual stress must be converted with equation (1) to the testing temperature and the stress-strain curve of the core material must be superposed. The supporting points for the stress-strain curves for every depth layer are the result and can be fitted with equation (2).

In Figure 3 (right), the supporting points and the resulting stress-strain curve (grey lines) are plotted in a three-dimensional illustration for every depth layer. Therefore, the supporting points and the stress-strain curves are shifted on the total strain axis to get the stress strain curves starting points in the point of origin of the depth axis.

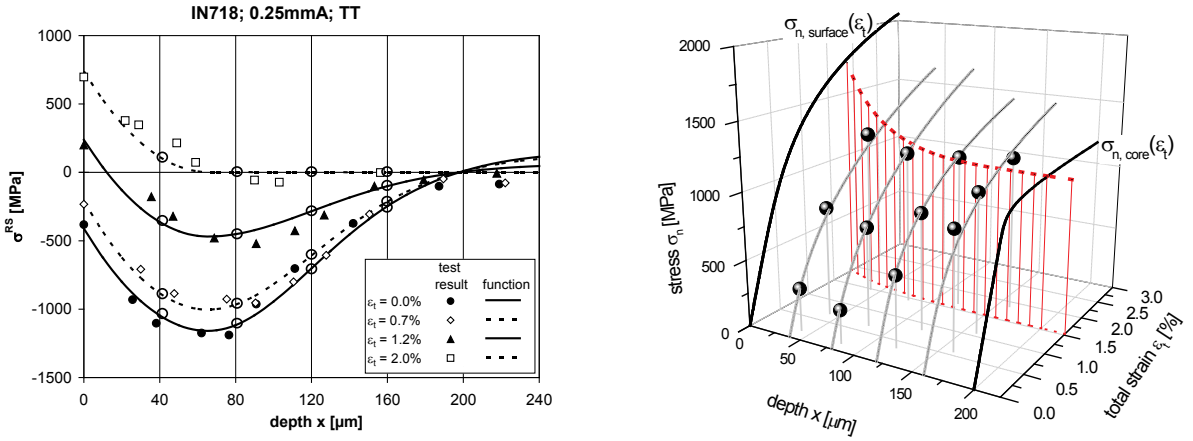

Figure 3: Different depth layers divided residual stress distributions (left) and the model of the different depth layers (right)

In this illustration, the hardening of the material decreases with increasing depth. At the surface (x = 0 µm) the stress-strain curve is correlating to the stress-strain curve at the surface (cf. Figure 2) and at a depth of about 200 µm it shows the stress-strain curve of the core material. The range between could be well described by the following equation (cf. Figure 3 right, red line):

$$R_{p,1\%}(x) = \left[\frac{x - x_0}{x_0}\right]^4 \cdot (R_{p,1\%,surface} - R_{p,1\%,core}) + R_{p,1\%,core} \quad for\ x < x_0$$
$$R_{p,1\%}(x) = R_{p,1\%,core} \quad for\ x \geq x_0 \qquad (3)$$

$R_{p,1\%}(x)$ is the technical elastic limit at 1 % plastic strain as a function of the depth x, $R_{p,1\%,surface}$ and $R_{p,1\%,core}$ are the technical elastic limit at 1 % plastic strain for the surface and the core and x_0 is the depth of zero crossing of the residual stress. This equation was deduced from the depth distribution of the full width at half maximum (FWHM), which is used as an indicator for work hardening. The FWHM distribution of the initial state shows the coherency (cf. Figure 4 (left)):

$$FWHM(x) = \left[\frac{x - x_0}{x_0}\right]^4 \cdot (FWHM_{surface} - FWHM_{coren}) + FWHM_{core} \quad for\ x < x_0$$
$$FWHM(x) = FWHM_{core} \quad for\ x \geq x_0 \qquad (4)$$

x_0 is the depth of zero crossing of the residual stresses, analogue to equation (3), $FWHM_{surface}$ and $FWHM_{core}$ are the full width at half maximum of the surface and the core.

To calculate the technical elastic limit $R_{p,1\%}$ the Ramberg-Osgood-approach is converted:

$$R_{p,1\%} = (0{,}01)^n \cdot K \qquad (5)$$

$R_{p,1\%}$ is thereby the technical elastic limit; K is the strain hardening coefficient and n the strain hardening exponent of the Ramberg-Osgood-approach.

By the aid of a further correlation which describes the strain hardening coefficient K or the strain hardening exponent n as function of the depth, it would be possible to describe the whole hardening of shot-peened specimens with the equations (3), (5), and the Ramberg-

Osgood-approach. The kind of function which is taken plays a secondary role because the technical elastic limit $R_{p,1\%}$ is given (cf. Equation (3)). Therefore a simple correlation was taken for the hardening coefficient K(x):

$$K(x) = \left|\frac{x - x_0}{x_0}\right| \cdot (K_{surface} - K_{core}) + K_{core} \quad for\ x < x_0$$
$$K(x) = K_{core} \quad for\ x \geq x_0 \tag{6}$$

$K_{surface}$ and K_{core} are the strain hardening coefficients of the surface and the core respectively, x_0 is the depth of the zero crossing of the residual stresses. The strain hardening exponent n(x) can be calculated with a transformed equation (5):

$$n(x) = \frac{log(R_{p,1\%}(x)) - log(K(x))}{log(0{,}01)} \tag{7}$$

After all the deformation behaviour as a function of the depth results (cf. Figure 4 (right)).

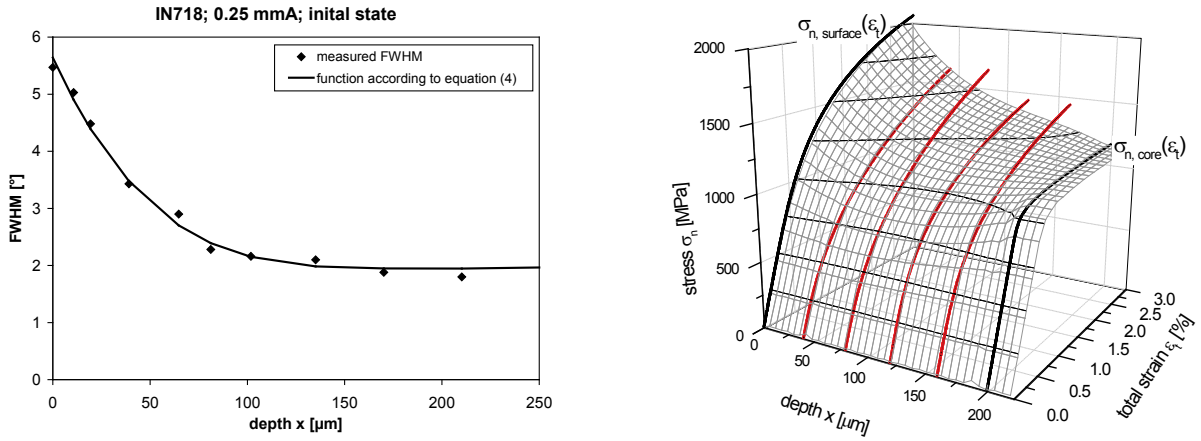

Figure 4: On the left the FWHM depth distribution of the initial state and equation (4) fitted to the test results and on the right the hardening as function of the depth and the total strain

So it's possible to calculate the residual stress depth distribution after a quasi-static mechanical loading condition. The result is shown in Figure 5 (left). The measured and the calculated residual stress depth distributions correlate very well.

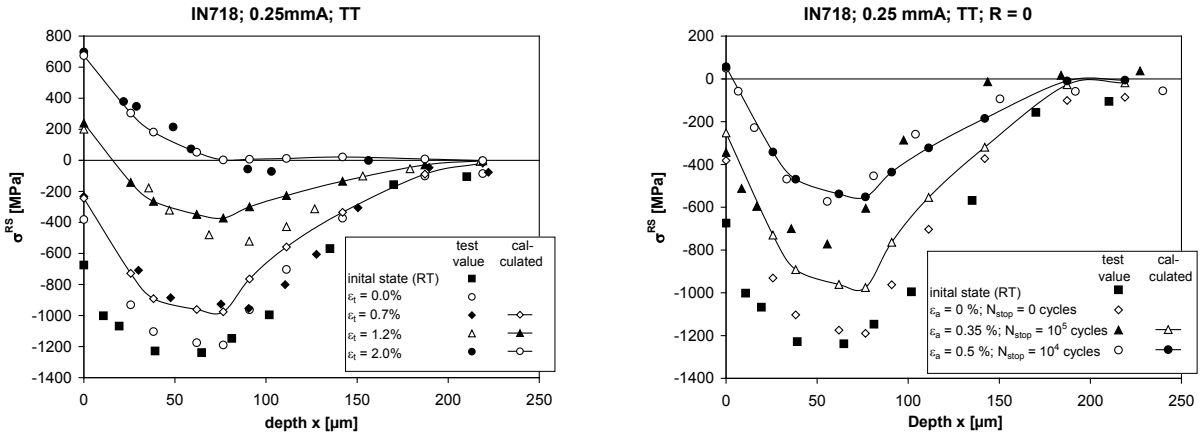

Figure 5: Measured and calculated residual stress depth distributions after different quasi-static (left) and cyclic (right) mechanical loading

Because the surface residual stresses show no dependence on the cycle number, it is assumed that only the quasi-static and not the cyclic elastic limit is exceeded [5]. So the model for the quasi-static loading condition could also be taken for the cyclic loading. In Figure 5 (right) the measured residual stress depth distribution is shown after different cyclic loadings and the distributions calculated with the quasi-static model. There is also a good correlation for the specimen which was loaded by a strain amplitude ε_a = 0.5 % at load ratio R = 0 and 10^4 cycles. For the state loaded with a strain amplitude ε_a = 0.35 % at load ratio R = 0 and 10^5 cycles there is a little mismatch. This mismatch could result either from the model or from variations in the shot-peening process.

Conclusion

The residual stress relaxation of shot peened IN718 after an isothermal quasi-static and cyclic loading was investigated by X-ray diffraction measurements. Therefore, different specimens were isothermally loaded with different total strains between 0 % and 2.5 % and isothermally cyclically loaded with a specific number of cycles and a total strain amplitude between 0.35 % and 0.6 % at fixed load ratio R = 0.

The compressive surface residual stresses decrease under quasi-static loading until tensile residual stresses are built up. The residual stress depth distributions show a similar behaviour. At cyclic loading, the residual stresses only change within the first cycle.

In order to describe quasi-static relaxation of the surface residual stresses and the residual stress depth distributions, the surface-core-model was extended to a multi-layer model. With this extended model, the experimental results can be well reflected in the whole impressed total strain range.

Because the residual stresses after cyclic loading are not dependent on the number of cycles, the quasi-static model can be applied also for cyclic residual stress changes.

References

[1] J. Hoffmeister, V. Schulze, A. Wanner, R. Hessert, G. König: Thermal Relaxation of residual Stresses induced by Shot Peening in IN718, In: K.Tosha (eds.), The 10th International Conference On Shot Peening, Tokyo, 2008, pp. 157-162.

[2] O. Vöhringer: Abbau von Eigenspannungen, In: V. Hauk E. Macherauch (eds.), Eigenspannungen, DGM-Informationsgesellschaft, Oberursel, 1983, pp. 49-83.

[3] O. Vöhringer: Relaxation of residual stresses by annealing or mechanical treatment, In: A. Niku-Lari (eds.), Advances in surface treatment; International Guidebook on Residual Stresses, Pergamon, New York, 1987, pp. 367-395.

[4] W. Ramberg, W. R. Osgood, NASA (non Center Specific): Description of stress-strain curves by three parameters, NACA Technical Note 902. (1943).

[5] E. Macherauch H. Wohlfahrt: Eigenspannungen und Ermüdung, In: D. Munz (eds.), Ermüdungsverhalten metallischer Werkstoffe, DGM-Informationsgesellschaft Verlag, Oberursel, 1985, pp. 237-283.